

The role of CYP46A1 and its metabolic product, 24S-hydroxycholesterol, in Neuro 2A cell death

Allen Ni¹, Xiangning Jiang²

¹Basis Independent Silicon Valley, San Jose, California

²Department of Neurology, University of California San Francisco, San Francisco, California

SUMMARY

Cholesterol is a major component of neuronal cell membrane and myelin sheath. Therefore, maintaining cholesterol homeostasis is crucial for brain functioning and development. Brain cholesterol is synthesized *de novo*. To achieve homeostasis, excess cholesterol is removed by its conversion into 24S-hydroxycholesterol (24S-HC), which crosses the blood-brain barrier to enter the blood stream for clearance. This conversion is facilitated by the brain-specific protein, CYP46A1 (cholesterol 24-hydroxylase). Previous studies reported that hypoxia-ischemia caused disruption of cholesterol homeostasis. Increases of CYP46A1 and 24S-HC in neonatal mouse brain correlated with hypoxic-ischemic brain damage. Blood level of 24S-HC was also elevated and is a potential diagnostic biomarker for brain damage severity. However, how CYP46A1 and 24S-HC are functionally involved in neuronal cell death is unknown. Finding the direct effect of CYP46A1 and 24S-HC on brain cell damage will help assess the possibility of using 24S-HC for brain damage diagnosis. We hypothesized that hypoxia-ischemia upregulated CYP46A1 expression, leading to an increase in 24S-HC, thus triggering cell death. In this study, we either transfected Neuro 2A cells with CYP46A1 cDNA or treated the cells with 24S-HC. Cell viability was measured to evaluate their effect on cell damage. Cells expressing CYP46A1 had significantly less viability compared to the negative control. Up to 55% reduction in cell viability was also observed in 24S-HC-treated cells. This work supports that CYP46A1 and 24S-HC could directly trigger cell death. The direct involvement of 24S-HC in cell death provides further evidence that 24S-HC can be a promising biomarker for diagnosing brain damage severity.

INTRODUCTION

Cholesterol plays an essential role in brain development and function (1). In fact, about 23% of human body cholesterol can be found in the brain even though the brain only occupies 2% of body mass (2). More than 70% of the brain cholesterol is used to form myelin sheath, a membrane structure that

is synthesized by oligodendrocytes to wrap around the axons. During myelination, a large quantity of cholesterol is accreted to reinforce the thickness of the hydrophobic membrane, which allows electric signals to travel rapidly through neurons over long distances (3). The rest of the brain cholesterol constitutes plasma membranes of brain cells and membranous subcellular organelles (2). In addition to its structural importance, brain cholesterol is critical in synaptogenesis, a process to form synaptic contact for neurotransmitter release and uptake between neurons (4).

Brain cholesterol synthesis is a separate process from the whole-body cholesterol metabolism (2, 5). There is no evidence that the cholesterol synthesized in peripheral tissues and carried in blood lipoproteins can pass through the blood-brain barrier (BBB), whose unique endothelial cells and tight junction sites selectively control the transportation of compounds from blood to brain (2, 5). On the other hand, local cholesterol synthesis in the brain is reported to occur at the same rate as cholesterol accumulation, which strongly suggests that the brain can make cholesterol to support its own use (5). A mechanism is also required to remove excess cholesterol from the brain to maintain appropriate cholesterol level. In this elimination process, cholesterol must be first converted into a more soluble substance called 24S-hydroxycholesterol (24S-HC), which can then cross the BBB and enter the bloodstream for further metabolization in the liver (6). This process is supported by the findings that the vast majority of 24S-HC in circulation originates from the brain (7). The enzyme, cholesterol 24-hydroxylase (CYP46A1), that carries out the hydroxylation conversion was cloned and identified as brain-specific, demonstrating that the brain is fully equipped with all necessary components to precisely regulate its cholesterol homeostasis (8). Disruption of cholesterol metabolism and accumulation of excess cholesterol are observed in neurodegenerative diseases such as Alzheimer's and Huntington's (1, 9). The alteration in cholesterol metabolism is also found to be associated with traumatic brain injury or hypoxia-ischemia-induced brain developmental disorder (10-11).

Hypoxic-ischemic encephalopathy is a type of brain injury caused by reduced oxygen and glucose supply to the brain. Hypoxia-ischemia occurring during the prenatal and perinatal development stages is the leading cause of infant mortality and life-long neurological defects, such as intellectual

disability and cerebral palsy in survivors (11). Magnetic resonance imaging (MRI) is a sensitive and commonly used imaging technique to diagnose infants with brain injury (12). MRI pattern, however, varies depending on multiple factors including imaging time, injury severity, and brain maturity, which could complicate an appropriate diagnosis (12). A fast, convenient, and reliable diagnosis tool for hypoxic-ischemic brain injury is therefore needed to directly measure parameters associated with brain cell death.

A recent report proposed that blood levels of 24S-HC could be used in diagnosing the severity of brain damage (13). This study used hypoxia-ischemia-induced neonatal mice. An increase of CYP46A1 expression and its product, 24S-HC, were detected in the mouse brain (13). Serum levels of 24S-HC were also elevated, which was not surprising considering its sole origin from brain and its permeability through the BBB. Furthermore, this increase correlated with brain damage, as evidenced by increased levels of spectrin-breakdown products (SBDPs) and cleaved caspase-3, respectively representing necrotic and apoptotic cell death (13). However, it is unknown whether and how CYP46A1 and its product 24S-HC are functionally involved in neuronal death.

We hypothesized that hypoxia-ischemia could induce CYP46A1 expression followed by an increased production

of 24S-HC, which then triggers cell death. In this study, we tested this hypothesis by investigating the effect of CYP46A1 overexpression and 24S-HC on neuronal-like cell damage. We demonstrated that a neuroblastoma cell line, Neuro 2A, had significantly reduced viability when CYP46A1 was overexpressed. 24S-HC treatment also directly caused Neuro 2A cell death. This work suggests the direct involvement of 24S-HC in Neuro 2A cell death, which supports its potential use as a candidate biomarker for diagnosing brain damage severity, allowing the possibility of faster and more reliable detection of brain damage.

RESULTS

Experimental design

We selected a mouse neuroblastoma cell line, Neuro 2A cells, to model neuronal cells in this *in vitro* study because of its neuronal origin and its morphology of neurons. More importantly, a previous study showed that Neuro 2A was equipped with the ability to synthesize cholesterol, the substrate for CYP46A1 (14). This property is crucial for our study as it allows us to examine the function of CYP46A1 and its product, 24S-HC, inside the cell line.

We performed two groups of experiments (**Figure 1**). In one group, plasmid DNA containing *CYP46A1* cDNA was

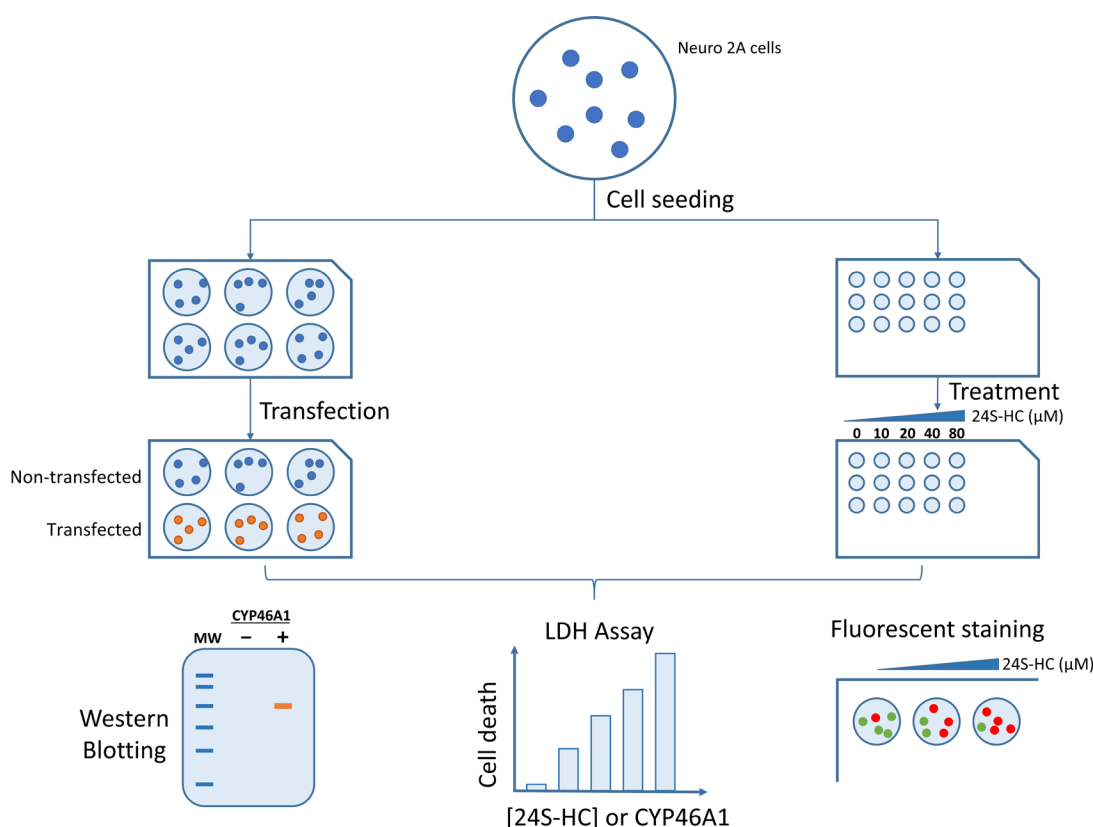


Figure 1. Diagram of experimental design. Neuro 2A cells were transfected with CYP46A1 cDNA followed by Western blotting to confirm the expression of the protein. Percent cell viability of CYP46A1-transfected cells and non-transfected cells was measured by LDH cytotoxicity assay. In a separate group, Neuro 2A cells were treated with 24S-HC at different concentrations. Cell viability was measured by either LDH cytotoxicity assay or a live/dead cell dual fluorescent staining. Three to four trials were performed in each group of experiments.

introduced into Neuro 2A cells to express CYP46A1. Western blotting was used to confirm the expression of the protein. In this experiment, the negative control was the cells that were transfected with transfection reagents only without plasmid DNA. We then measured percent cell viability of CYP46A1-transfected cells and non-transfected cells by lactate dehydrogenase (LDH) cytotoxicity assay. In the other group, we treated Neuro 2A cells with 24S-HC at different concentrations (0 μ M, 20 μ M, 40 μ M, 60 μ M, 80 μ M). The negative control was the non-treated cells. The cells from the 24S-HC treatment were then tested for their cell viability using LDH cytotoxicity assay or a LIVE/DEAD fluorescent assay. Three to four trials were performed in each group of experiments.

CYP46A1 overexpression reduced Neuro 2A cell viability

To investigate if CYP46A1 causes neuronal-like cell death, we transfected mouse Neuro 2A cells with a plasmid containing human *CYP46A1* cDNA (pCMV-FLAG-CYP46A1, **Figure 2A**) (15). Human and mouse *CYP46A1* sequences are 94.8% identical. This same plasmid was previously used in rat neurons to show that the translated CYP46A1 protein was functional (15). Human *CYP46A1* was fused in-frame with a FLAG tag at the 5' end. Gene transcription was initiated by

the cytomegalovirus (CMV) promoter. To confirm the protein was expressed, western blotting (WB) was conducted using mouse anti-CYP46A1 antibody (**Figure 2B**). We observed a band matching the molecular weight of CYP46A1 (57 kDa) in transfected cells. The same band, as expected, was absent from non-transfected Neuro 2A cells. β -actin, a housekeeping protein, was used as the loading control. Co-incubation of anti- β -actin antibody detected a 42 kDa band present in both transfected and non-transfected cell lysate, showing equal loading of protein. This validated that the Neuro 2A cells were successfully transfected and that the introduction of pCMV-FLAG-CYP46A1 plasmid led to successful expression of CYP46A1.

We then examined if overexpression of CYP46A1 had any effect on cell viability by transfecting Neuro 2A cells with 0.5 μ g pCMV-FLAG-CYP46A1 plasmid. Three days after transfection, cell viability was measured by LDH cytotoxicity assay. Cells transfected with 0.5 μ g plasmid showed lower average viability at 66% (n=3) cell viability compared to corresponding non-transfected cells with an average viability of 78% (**Figure 2C**). This difference was statistically significant ($p < 0.05$, unpaired t-test). To study if the reduction in cell viability was dosage dependent on CYP46A1, we then transfected the cells with double the amount of pCMV-

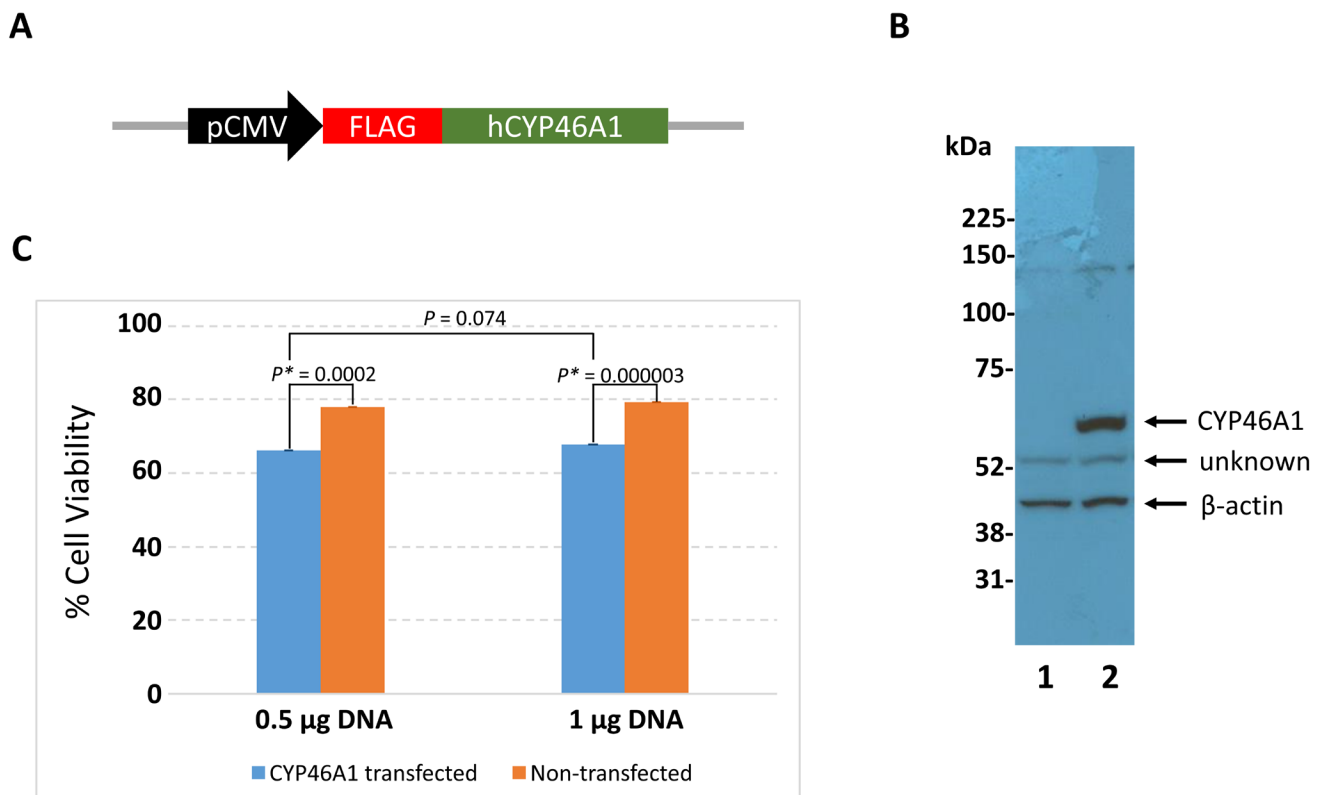


Figure 2. Overexpression of CYP46A1 significantly increased cell death. **A)** Partial construct of the plasmid vector containing human *CYP46A1* (15). **B)** Overexpression of CYP46A1 protein as detected by Western blotting. Lane 1: non-transfected cell lysate; lane 2: pCMV-FLAG-CYP46A1-transfected cell lysate. β -actin was used to control loading. **C)** Average percent cell viability of Neuro 2A cells transfected with pCMV-FLAG-CYP46A1 at different DNA amounts. Blue bar: cells transfected with pCMV-FLAG-CYP46A1 at 0.5 μ g or 1 μ g; orange bar: non-transfected cells. Mean \pm standard deviation is shown (n = 3). P -value was labeled to show statistical significance; unpaired t-test.

FLAG-CYP46A1 (1 µg). A similar result was observed where 68% of CYP46A1-transfected cells survived, while the non-transfected cells showed a higher viability at 79% (**Figure 2C**). Transfection with different pCMV-FLAG-CYP46A1 amounts (0.5 µg and 1.0 µg) did not result in significant differences in cell viability.

24S-HC-induced Neuro 2A cell death in a dose-dependent manner

A previous study reported that 24S-HC levels increased up to 100 µM in hypoxia-ischemia-induced mouse brain (13). Based on this information, we treated separate samples of Neuro 2A cells with 24S-HC at increasing concentrations from 0 µM to 80 µM for 16 hours. Live and dead cells were visualized by dual fluorescence staining (**Figure 3A**), in which live healthy cells were labeled green by calcein, while dead

cells were stained red by ethidium homodimer-1 (EthD-1). Without 24S-HC (0 µM), almost all cells were labeled green, indicating little cell damage. After adding increasing concentrations of 24S-HC, we started to see cell death represented by red-stained cells. The increase in population of red cells was dose-dependent, in which more than half of the cells were labeled red when 24S-HC concentration reached 80 µM (the highest tested concentration). Cells were viewed under different fluorescent filters and images were overlaid to demonstrate discrete fluorescent staining between live and dead cells (**Figure 3B**).

Cell death was further quantified as % cell viability = $100 \times \left[\frac{\# \text{ of green cells}}{\# \text{ of green cells} + \# \text{ of red cells}} \right]$. We found that 99.7% of cells were viable without 24S-HC treatment (**Figure 3C**, blue line). There was a slight decrease in cell viability when 24S-HC concentration was increased to 10 µM.

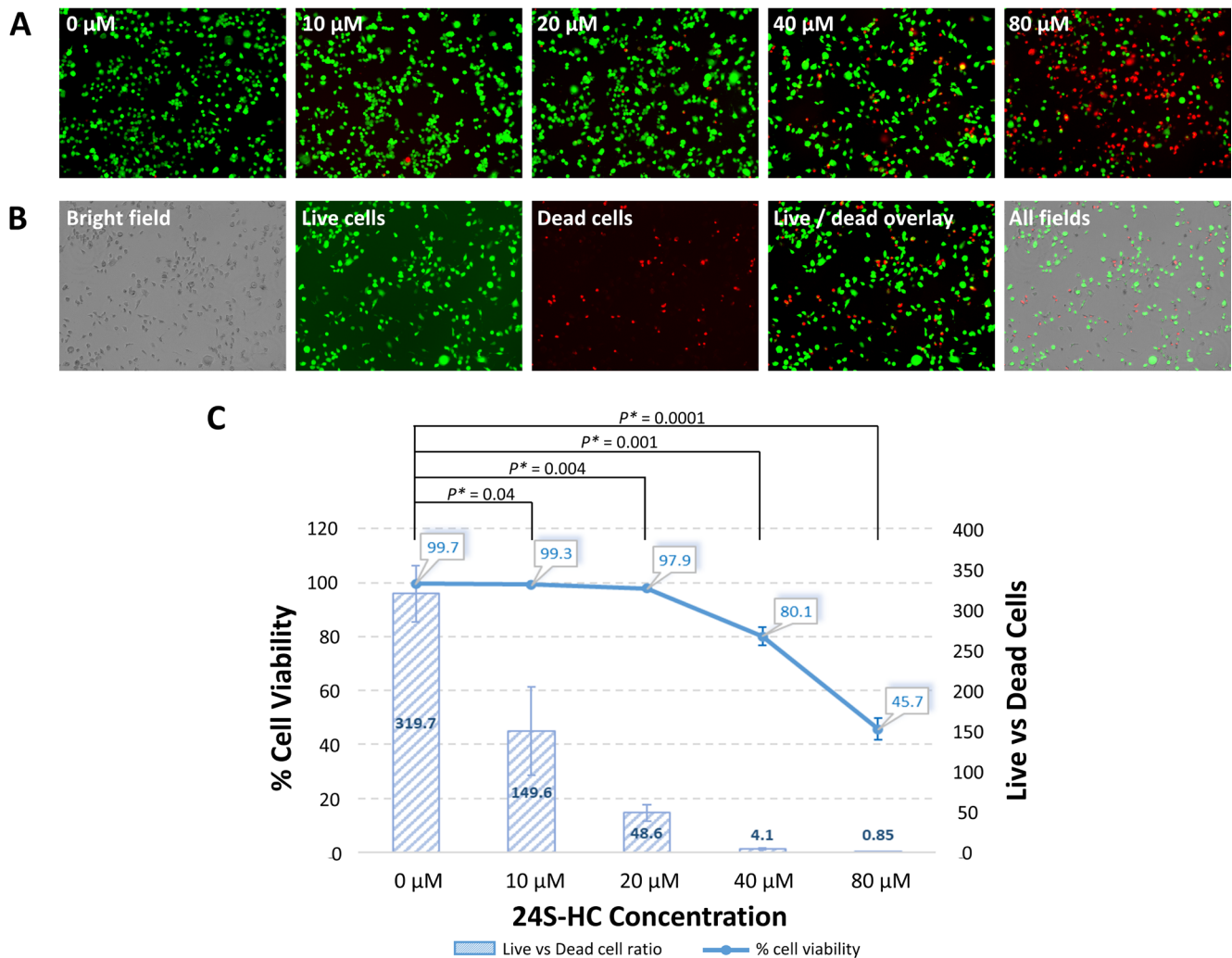


Figure 3. 24S-HC treatment caused a significant dose-dependent increase of cell death. **A)** Dual fluorescent staining to show population of live cells (green) and dead cells (red) at different 24S-HC concentrations. Representative images from one sample of each treatment condition were shown. **B)** Cells observed under bright-field and fluorescent microscopy. Representative images from 40 µM 24S-HC treatment were shown. **C)** Average Neuro 2A cell death under different treatment concentrations. Blue line: percent cell viability measured by percentage of live cell number over total cell number; blue bar: ratio of live cells to dead cells. Mean ± standard deviation is shown (n=4). P-value was labeled to show significance of differences between treated vs non-treated samples; unpaired t-test.

This decrease was statistically significant ($p = 0.04$, unpaired t-test). A continuous increase in 24S-HC concentration led to more cell death as shown by the drastic increase in the negative slope of the blue line. Neuro 2A cells treated with 80 μM 24S-HC had the lowest average viability at 45.7% ($n=4$).

We also reviewed cell death by the ratio of live-to-dead cells (Figure 3C, blue bars). Live-to-dead cell ratios started to drop at 10 μM concentration and continued to drop while 24S-HC concentration increased. At 80 μM , live-to-dead cell ratio was < 1 , meaning that more than half of the cells were dead. All concentrations of 24S-HC resulted in significant cell death as compared with the control.

24S-HC induced Neuro 2A cell death in time-dependent manner

A recent publication reported that CYP46A1 was dramatically upregulated at 6 hours after hypoxic-ischemic challenge (13). 24S-HC level in brain and serum was concurrently increased, correlating with a rise in cell death as measured by apoptotic markers (13). To study the time effect of 24S-HC on cell death in the current model, we subjected Neuro 2A to a shorter treatment of 5 hours in addition to 16 hours. We then measured the cell viability by a LDH cytotoxicity assay. During the 5-hour incubation, Neuro 2A cells did not show a significant change in cell viability across the tested range of 24S-HC concentrations (Figure 4, orange line) ($p > 0.05$ at 80 μM , unpaired t-test). In contrast, the 16-hour treatment resulted in a drastic decrease of viable cells from 100% to 44.58% when 24S-HC rose from 0 to 80 μM (Figure 4, blue line) ($p < 0.05$ at 80 μM , unpaired t-test). Moreover, percent cell viability from the 16-hour treatment determined by LDH activity showed a pattern of downward drop similar to the results measured by the live/dead cell fluorescent staining method.

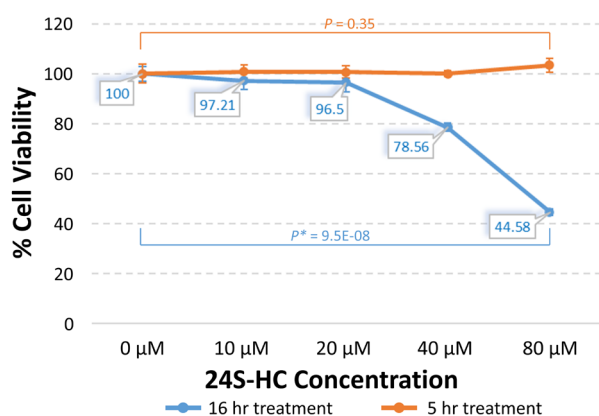


Figure 4. 24S-HC induced Neuro 2A cell death in time-dependent manner. Average percent cell viability was measured by LDH cytotoxicity assay. Blue line: 16-hour treatment with 24S-HC; orange line: 5-hour treatment with 24S-HC. Mean \pm standard deviation is shown ($n=4$). P -value was labeled to show significance of differences at 80 μM treatment; unpaired t-test.

DISCUSSION

We chose to use Neuro 2A in this study because of its ability to synthesize cholesterol (14). Additionally, our experiment demonstrated that Neuro 2A did not have detectable, naturally existing CYP46A1 by WB (Figure 2B, non-transfected), which guarantees that the artificially introduced CYP46A1 is the sole factor in causing cell death. In addition, the immortal nature of Neuro 2A provides convenience for easy and continuous culture and consistency in results.

Even though the Neuro 2A cell line has its advantages to fit the purpose of this study, it differs biologically from highly specialized neuronal primary cells. For example, Neuro 2A was found to have different sensitivity to neurotoxins compared to primary cells (16). As a result, the effective concentration of 24S-HC and treatment time course may need further study in primary neurons and *in vivo*. It is also worthwhile to find out the target molecule of 24S-HC that triggers cell death.

A previous study demonstrated that CYP46A1 was upregulated in hypoxia-ischemia-induced neonatal mice (13). The elevation in CYP46A1 expression lasted for up to 48 hours and correlated with increased levels of SBDPs and cleaved caspase-3, both of which represented necrotic and apoptotic cell death (13). However, it remains unclear how CYP46A1 was activated and involved in cell death. In our experiment, introduction of CYP46A1 into Neuro 2A triggered cell death. This effect may be achieved via converting cholesterol to 24S-HC which in turn caused cell death. Measurement of 24S-HC generation in CYP46A1 transfected cells would confirm this hypothesis in the future study. Whether CYP46A1 affects brain damage in the same way *in vivo* is another interesting aspect for future research. This could be done by using CYP46A1 knockout mice or a CYP46A1 specific inhibitor.

In this *in vitro* study, we examined 24S-HC treatment at concentrations ranging from 0–80 μM . It would be interesting to further explore whether 24S-HC concentration in brain tissue after hypoxic-ischemic induction reaches a similar level. A report showed that 6 hours after hypoxic-ischemic induction, mouse neonatal brain tissue had increased levels of 24S-HC at 40 ng/mg wet weight, correlating with signs of brain damage (13). Considering mouse brain density of 1.04 g/mL (17) and 24S-HC molecular weight of 403 g/mol, 40 ng/mg of 24S-HC is equivalent to 100 μM , which is close to the highest concentration tested in this study. Unlike the *in vivo* mouse model, however, our *in vitro* study did not see any effect on cell death when Neuro 2A cells were treated with 24S-HC for 5 hours. More than 50% cell death was only elicited after prolonging the treatment to 16 hours with 80 μM 24S-HC. This could be explained by the difference between *in vitro* versus *in vivo* and between brain tumor cell line versus primary cells, which further strengthens the need for *in vivo* and primary cell testing.

The current study demonstrated that introduction of CYP46A1 or 24S-HC was able to directly induce cell death in the Neuro 2A cell model. Specifically, 80 μM of 24S-HC caused $>50\%$ cell death after 16 hours of treatment. Similar

levels of 24S-HC were detected in hypoxic-ischemic injured neonatal mouse brain. The direct involvement of 24S-HC and CYP46A1 in cell death provides rationale for using 24S-HC as a biomarker to diagnose brain damage severity.

METHODS

Cell culture and transfection

Neuro 2A cells (CCL-131, ATCC) were cultured in Dulbecco's Modified Eagle Medium (DMEM; 10569044, Thermo Scientific) supplemented with 10% fetal bovine serum (FBS; 16140071, Thermo Scientific) and penicillin (100 U/mL)–streptomycin (100 ug/mL) antibiotics (15140122, Thermo Scientific). Cells were cultured in a 37°C incubator with 5% CO₂. For transfection, Neuro 2A cells were seeded in 6-well plates. Three days after seeding, pCMV-FLAG-CYP46A1 (15) was transfected into Neuro 2A cells using Lipofectamine 3000 kit (L3000015, Thermo Scientific). Transfected cells were cultured for three more days followed by analysis of protein expression and cell viability. In the negative control, Neuro 2A cells were transfected with transfection reagents only without pCMV-FLAG-CYP46A1.

Western blotting

Cells were lysed in RIPA buffer (R0278, Millipore). Protein concentration was measured by BCA kit (23225, Thermo Scientific). Equal amounts of protein lysate were loaded onto 4–12% Bis-Tris SDS polyacrylamide gel to separate the protein by size. Proteins were transferred to polyvinylidene difluoride (PVDF) membrane which was then incubated in TBS + 0.05% Tween-20 and 5% milk to block nonspecific binding sites. Membrane was blotted with mouse anti-CYP46A1 antibody at 1:1,000 (1A7, MAB2259, Millipore) and anti-β-actin antibody followed by goat anti-mouse HRP conjugate at 1:1,000 (Santa Cruz Biotechnology). The protein bands were visualized by chemiluminescence on X-ray film.

Cell treatment with 24S-HC

Neuro 2A cells were seeded into 24-well plates and cultured for two days. Once reaching 80% confluence, culture medium was replaced with treatment medium, which was DMEM (no phenol red) containing 24S-HC diluted to concentrations ranging from 0–80 μM. DMEM without phenol red was used to avoid interference in LDH assay. Treated cells were continuously cultured at 37°C for 5 hours or 16 hours.

LDH cytotoxicity assay

LDH is a cytosolic enzyme produced in cells. If the cell membrane breaks, LDH is released into the medium, indicating cell death. LDH activity was measured by LDH cytotoxicity detection kit (MK401, Takara). Cell culture supernatant from either transfected or treated cells was collected and tested for LDH activity that was released from the dead cells because of transfection or treatment. The remaining live cells in the plate were frozen and thawed in equal volumes of fresh

culture medium to release LDH. Percent cell viability was calculated as $100 \times [\text{LDH A490}_{\text{live cells}} / (\text{LDH A490}_{\text{live cells}} + \text{LDH A490}_{\text{dead cells}})]$. The higher amount of LDH activity in the culture supernatant indicated higher percentage of cell death.

LIVE/DEAD cells fluorescent staining

24S-HC-treated cells were stained by the dye mixture using LIVE/DEAD viability kit (L3224, Thermo Scientific). After 45 min incubation at 37°C, staining was visualized under fluorescent microscope. Live, healthy cells were labeled green after non-fluorescent calcein-AM penetrated through cell membrane and converted to green, fluorescent calcein by intracellular esterases. Dead cells were stained red with ethidium homodimer-1 (EthD-1) because dead cells lose their membrane integrity allowing EthD-1 to enter the cell and bind to the DNA. % cell viability = $100 \times [\# \text{ of green cells} / (\# \text{ of green cells} + \# \text{ of red cells})]$.

Statistical analysis

Percent cell viability and live-to-dead cell ratio were expressed as mean ± standard deviation. Unpaired t-test was used to evaluate if the difference in cell viability was significant after cells were introduced with different pCMV-FLAG-CYP46A1 amounts or treated with 24S-HC at various concentrations for different treatment time. $P < 0.05$ was considered statistically significant.

ACKNOWLEDGEMENTS

We thank Dr. Fuxin Lu, for his support, guidance, and teaching throughout the entire work. This work was supported by NINDS grant 1R56NS114563-01A1.

Received: October 9, 2020

Accepted: March 13, 2021

Published: May 11, 2021

REFERENCES

1. Zhang, Juan, and Qiang Liu. "Cholesterol Metabolism and Homeostasis in the Brain." *Protein & Cell*, vol. 6, no. 4, 2015, pp. 254–264., doi:10.1007/s13238-014-0131-3.
2. Dietschy, John M. "Central Nervous System: Cholesterol Turnover, Brain Development and Neurodegeneration." *Biological Chemistry*, vol. 390, no. 4, 2009, doi:10.1515/bc.2009.035.
3. Saher, Gesine, *et al.* "High Cholesterol Level Is Essential for Myelin Membrane Growth." *Nature Neuroscience*, vol. 8, no. 4, 2005, pp. 468–475., doi:10.1038/nn1426.
4. Mauch, Daniela H. "CNS Synaptogenesis Promoted by Glia-Derived Cholesterol." *Science*, vol. 294, no. 5545, 2001, pp. 1354–1357., doi:10.1126/science.294.5545.1354.
5. Dietschy, John M., and Turley, Stephen D. "Cholesterol metabolism in the central nervous system during early development and in the mature animal." *Journal of Lipid*

- Research*, vol. 45, no. 8, 2004, pp. 1375-1397., doi: 10.1194/jlr.R400004_JLR200
6. Russell, David W., *et al.* "Cholesterol 24-Hydroxylase: An Enzyme of Cholesterol Turnover in the Brain." *Annual Review of Biochemistry*, vol. 78, no. 1, 2009, pp. 1017–1040., doi:10.1146/annurev.biochem.78.072407.103859.
 7. Björkhem, Ingemar, *et al.* "Cholesterol homeostasis in human brain: turnover of 24S-hydroxycholesterol and evidence for a cerebral origin of most of this oxysterol in the circulation." *Journal of Lipid Research*, vol 39, no. 8, 1998, pp. 1594-1600.
 8. Lund, Erik G., *et al.* "CDNA Cloning of Cholesterol 24-Hydroxylase, a Mediator of Cholesterol Homeostasis in the Brain." *Proceedings of the National Academy of Sciences*, vol. 96, no. 13, 1999, pp. 7238–7243., doi:10.1073/pnas.96.13.7238.
 9. Hudry, Eloise, *et al.* "Adeno-Associated Virus Gene Therapy with Cholesterol 24-Hydroxylase Reduces the Amyloid Pathology Before or After the Onset of Amyloid Plaques in Mouse Models of Alzheimer's Disease." *Molecular Therapy*, vol. 18, no. 1, 2010, pp. 44–53., doi:10.1038/mt.2009.175.
 10. Cartagena, Casandra M., *et al.* "24S-Hydroxycholesterol Effects on Lipid Metabolism Genes Are Modeled in Traumatic Brain Injury." *Brain Research*, vol. 1319, 2010, pp. 1–12., doi:10.1016/j.brainres.2009.12.080.
 11. Vannucci, Susan J. "Hypoxia-Ischemia in the Immature Brain." *Journal of Experimental Biology*, vol. 207, no. 18, 2004, pp. 3149–3154., doi:10.1242/jeb.01064.
 12. Varghese, Binoj, *et al.* "Magnetic resonance imaging spectrum of perinatal hypoxic-ischemic brain injury." *The Indian Journal of Radiology and Imaging*, vol. 26, no. 3, 2016, pp. 316-327., doi: 10.4103/0971-3026.190421.
 13. Lu, Fuxin, *et al.* "Upregulation of Cholesterol 24-Hydroxylase Following Hypoxia–Ischemia in Neonatal Mouse Brain." *Pediatric Research*, vol. 83, no. 6, 2018, pp. 1218–1227., doi:10.1038/pr.2018.49.
 14. Korade Željka, *et al.* "Molecular Consequences of Altered Neuronal Cholesterol Biosynthesis." *Journal of Neuroscience Research*, vol. 87, no. 4, 2009, pp. 866–875., doi:10.1002/jnr.21917.
 15. Moutinho, Miguel, *et al.* "Neuronal Cholesterol Metabolism Increases Dendritic Outgrowth and Synaptic Markers via a Concerted Action of GGase-I and Trk." *Scientific Reports*, vol. 6, no. 1, 2016, pp. 1-18., doi:10.1038/srep30928.
 16. Lepage, Keith T., *et al.* "On the Use of Neuro-2a Neuroblastoma Cells Versus Intact Neurons in Primary Culture for Neurotoxicity Studies." *Critical Reviews™ in Neurobiology*, vol. 17, no. 1, 2005, pp. 27–50., doi:10.1615/critrevneurobiol.v17.i1.20.
 17. Leithner, Christoph, *et al.* "Determination of the Brain-Blood Partition Coefficient for Water in Mice Using MRI." *Journal of Cerebral Blood Flow and Metabolism*, vol. 30, no. 11, 2010, pp. 1821-1821., doi: 10.1038/jcbfm.2010.160.

Copyright: © 2021 Ni and Jiang. All JEI articles are distributed under the attribution non-commercial, no derivative license (<http://creativecommons.org/licenses/by-nc-nd/3.0/>). This means that anyone is free to share, copy and distribute an unaltered article for non-commercial purposes provided the original author and source is credited.